Bull. Chem. Soc. Jpn., **68**, 696—712(1995)

Accounts

Effects of the Solvent Dynamics and Vibrational Motions in Electron Transfer

Keitaro Yoshihara,* Keisuke Tominaga, and Yutaka Nagasawa

Institute for Molecular Science, Myodaiji, Okazaki 444

(Received November 22, 1994)

Recent theoretical and experimental progress concerning electron transfer (ET) in solution is reviewed by focusing on the mechanism of ET, which occurs much faster than solvation dynamics. Theories of ET in solution are briefly reviewed with particular emphasis placed on the relation to solvent dynamics. Experimental methods to investigate solvent polarization relaxation are described. Ultrafast *intramolecular* ET, which is found in back ET from the photo-induced charge-transfer state to the ground state, is described concerning highly polar betaines and mixed-valence compounds. Ultrafast *intermolecular* ET has been observed for the systems of various dyes in electron-donating solvents. A non-exponential process with a significant temperature dependence was observed in aniline. A faster ET with a single exponential decay as fast as 10^{13} s^{-1} was observed with no temperature dependence in a system of oxazine 1 in *N*,*N*-dimethylaniline. The ET rate constants of excited coumarins in electron-donating solvents drastically depend on the substituent groups of the coumarin. Relatively small Stokes shifts in steady-state fluorescence spectra of ultrafast reacting molecules in solution are evidence of a "chemical timing" effect; namely, the reaction occurs in a non-equilibrium configuration of the solvent. These experimental observations are explained in terms of the extended Sumi–Marcus theory, in which the effect of solvation dynamics and low- and high-frequency vibrational modes are taken into account.

Electron transfer (ET) is one of the most common reactions in both chemistry and biology. Oxidation and reduction reactions are one form of ET, and appear in the redox reactions of transition-metal ions and complexes as well as organic compounds. ET triggers polymerization reactions, photography, electrochemistry, photosynthesis, metabolism, and many other processes. This ubiquitous nature and relative simplicity have made it a subject of extensive research for many years. Classical ET theories were most successfully developed on the basis of transition-state theory (TST) during the 1950's and 60's (for example see Refs. 1, 2, 3, and 4). This has been widely applied to many different types of molecular and biomolecular systems along with further developments of our theoretical understanding of the effects of the vibrational modes on ET.[3—7] More recently, the dynamical effects of nuclear motions on ET have received wide attention, and extensive theoretical research has been carried out.[5—23] Recent developments of ultrafast spectroscopies have enabled us to observe ET processes more directly, and a few experimental observations on the dynamical effects of nuclei have been reported for certain intra- and intermolecular ET systems.

In this article, recent developments on the dynamical aspects of ET in solution are reviewed. Usually, the electric dipole moment of a reactant species is changed by ET, which requires a rearrangement of the dielectric polarization of the solvents surrounding the reactant. This reorganization occurs on a finite time scale. Let us choose experimentally available parameters, namely, the rate constant of ET (k_{ET}) and the solvent relaxation time (τ_s), and then discuss the mechanism of ET in relation to these parameters. This is not simple in practice, since k_{ET} consists of not only a pre-exponential factor, but also an activation term. There are a few parameters used to describe solvent relaxation processes. With these facts in mind, we would like to overview the theoretical treatments on the dynamics of ET.

1) When the rate of ET is much slower than solvent relaxation ($k_{ET} \ll \tau_s^{-1}$) we can safely assume that a quasi-equilibrium condition between the reactant state and the transition state holds, and thus the fundamental assumption of TST is also safely satisfied.[1—4] The electronic interaction in this case is usually weak compared to any other free-energy parameters (free-en-

ergy difference and reorganization energy), and ET is a non-adiabatic process. The solvent is usually treated as a static dielectric medium. A quantum mechanical theory including the effects of a high-frequency vibrational mode on ET was worked out using perturbation theory.[5—7] 2) When there is an electronic interaction between two interacting potentials, namely the reactant and the product, the adiabaticity increases. If they are of the same order ($k_{ET} \approx \tau_s^{-1}$), the ET rate constant is inversely proportional to the solvent relaxation times and is restricted by the solvent relaxation time. ET becomes a "solvent-controlled reaction".[8—12,15—22] 3) If ET is faster than the solvent relaxation time ($k_{ET} > \tau_s^{-1}$) the above arguments become invalid and the effect of much faster motions, such as high-frequency intermolecular motions and intramolecular motions, play important roles in the dynamical processes. When different types of motions are competing with each other, a reaction in the non-equilibrium configuration of the solvent is expected. 4) When ET is very much faster than the solvent relaxation process ($k_{ET} \gg \tau_s^{-1}$) the solvent motions are completely frozen and solvent dynamics have no role in ET.

In the present article we discuss recent progress concerning theories and experiments of ET faster than the solvation dynamics in light of the effects of solvent dynamics and vibrational excitation. As for experiments, we mainly focus on *intramolecular* ET studied by Barbara and coworkers[24—32] as well as *intermolecular* ET studied by us.[33—41] Both of the experimental results are critically compared with theoretical predictions based on a new model in which solvation dynamics and vibrational excitation play important roles in the ET. In section I, theories of ET are briefly summarized. A description of the solvent relaxation process is given in section II. In section III, ultrafast intramolecular ET is described with organic and inorganic ions. Section IV is devoted to intermolecular ET between excited dye molecules and electron-donating solvents.

I. Theory of Electron Transfer

I-1. Non-Adiabatic Electron Transfer. The theory of ET in solution has been summarized and reviewed in many articles.[1—23,42] In the present section we briefly summarize the relevant concepts and equations, which will serve as a basis for a comparison with experiments. To derive an expression for the rate constant of ET we first start from a non-adiabatic treatment, and then extend the theory so as to be applicable to more general cases. Let us begin with transition-state theory (TST). ET is a subject of free-energy surface crossing from a reactant energy surface to a product one, just as in any other chemical reaction. The fundamental assumption of TST is that the reactant is kept under quasi-equilibrium with the transition state during the reaction. For a simple linear reaction (A→B) the reaction rate constant (k_{TST}) can be written as

$$k_{TST} = \frac{p\omega_0}{2\pi} \exp\left(-\frac{\Delta G^*}{k_B T}\right), \quad (1)$$

where ω_0 is the frequency of motion in the reactant potential well, ΔG^* the free energy of activation, p the electronic-transition probability at the transition region and $k_B T$ the thermal energy. Nuclear motions of the solvent and reactant molecules are in thermal equilibrium before the reaction. Once a large fluctuation of the solvent nuclear motion brings the reactant to the transition state, a reaction takes place according to probability p. Then, any excess energy will be disposed of into the solvent heat bath, and the whole system relaxes to a new equilibrium for the product. In some cases ET does not occur in the gas phase, but does occur in a polar solvent. One of the interactions which should be considered in ET is a dielectric interaction between an electric dipole moment of the reactant species and the reaction field induced by this dipole in the surrounding solvent. To describe the free-energy surface for ET a solvent coordinate is often used, which describes the collective motion of the solvent molecules and corresponds to the solvent polarization. The reorganization dynamics of the solvent are often treated sufficiently fast compared to the other dynamics involved in the reaction.

The probability (p) is a function of the electronic matrix element (V_{el}) in the case of ET. V_{el} is approximately proportional to an overlap integral between the wave functions of the reactant and the product. When V_{el} is small, the free-energy surface becomes non-adiabatic; when it is large, the surface becomes adiabatic. In the non-adiabatic case, the rate of ET can be written as[3]

$$k_{NA} = \frac{2\pi}{\hbar} \frac{V_{el}^2}{\sqrt{4\pi\lambda_s k_B T}} \exp\left(-\frac{\Delta G^*}{k_B T}\right), \quad (2)$$

where λ_s is the solvent reorganization energy, defined in Fig. 1 (λ in Fig. 1).

Under the assumption of a linear response of the dielectric interaction between the reactant species and the surrounding solvent the free-energy functions of the reactant and the product can be expressed in terms of a quadratic function of the solvent coordinate with the same curvature, and the activation energy can be simply described by[1—3]

$$\Delta G^* = \frac{(\lambda_s + \Delta G_0)^2}{4\lambda_s}, \quad (3)$$

with a free-energy gap (ΔG_0) between the product and the reactant states. The energy-gap dependence of the ET rate constant can be separated into the following three regions: (a) $-\Delta G_0 < \lambda_s$, the region where the reaction becomes faster as $-\Delta G_0$ increases. (b) $-\Delta G_0 = \lambda_s$, the reaction occurs fastest because the activation barrier vanishes. The free-energy surface of the product crosses the bottom of the reactant surface. (c) $-\Delta G_0 > \lambda_s$, the reaction becomes slower again as $-\Delta G_0$ increases. Therefore, the rate constant shows a bell-shaped dependence on the free-energy gap. Case

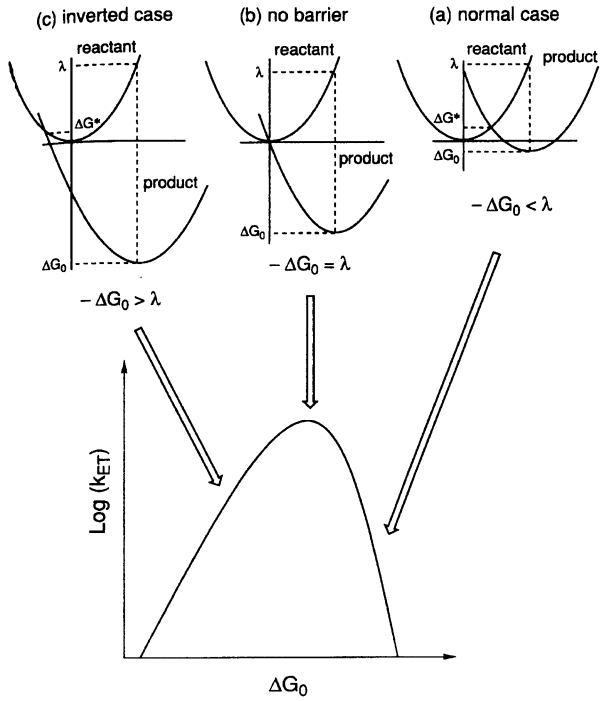

Fig. 1. Energy-gap dependence of electron transfer rate constant k_{ET} and its relation to the relative position of the free energy surfaces of reactant and product.

(a) is called the "normal region", and (c) is called the "inverted region". Many experimentalists have tried in vain to confirm the prediction of Marcus with donor-acceptor combinations in solution until recent observations. These have involved donor and acceptor moieties separated by a rigid spacer with a steroid structure,[43,44] ET between the adsorbate and the substrate,[45,46] a charge shift between organic ions and neutrals at cryogenic temperature,[47] and charge recombination reactions of ion radical pairs.[48—51]

I-2. Effects of a High-Frequency Vibrational Mode. So far, we have mainly treated ET as being an event between two electronic states, and considered the effects of solvent reorganization on the reaction. A contribution of intramolecular degrees of freedom has been ignored. Intramolecular motions include high-frequency quantized vibrational modes, which provide multiple reaction channels. The high-frequency quantum mode is particularly important in the inverted region, as shown in Fig. 2. The ground state of the reactant has a good vibrational overlap with a few vibrational states of the product. The ET rate constant becomes larger in the inverted region, compared to the normal region, and makes the bell-shape become asymmetric. This effect has actually been observed in the long-distant ET of a separated donor and acceptor by an inert rigid spacer.[43,44]

The effect of high-frequency vibrational modes can be incorporated by generalizing the non-adiabatic expression, Eq. 2.[3] The overall rate constant is the sum over

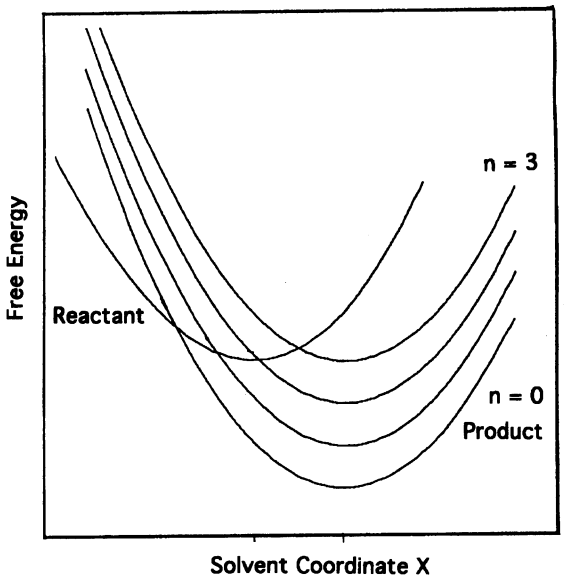

Fig. 2. A free energy surface crossing in the "inverted region" showing efficient contribution of the high frequency vibrational modes of the product surface, which makes the "bell shape" of the free energy dependence of electron transfer asymmetric.

all of the individual rate constants for different vibronic channels,

$$k_{NA} = \sum_n k_{NA}^{0\to n}. \tag{4}$$

Here, $k_{NA}^{0\to n}$ is the non-adiabatic rate constant between the ground vibrational state of the reactant and the n-th excited vibrational state of the product. We assume that the reaction takes place from the ground vibrational state of the reactant. $k_{NA}^{0\to n}$ has a similar functional form as that of the non-adiabatic expression Eq. 2 except for the effective energy gap, which takes into account of the quantization of energy,

$$\Delta G_0^{0\to n} = \Delta G_0 + nh\nu, \tag{5}$$

and the effective electronic matrix element, which considers the Franck–Condon overlap between two vibronic states,

$$(V_{el}^{0\to n})^2 = V_{el}^2 |\langle 0 \mid n\rangle|^2. \tag{6}$$

The Franck-Condon factor is expressed as

$$|\langle 0 \mid n\rangle|^2 = (S^n/n!)\exp(-S), \tag{7}$$

where the electron vibrational coupling strength (S) is given by

$$S = \lambda_{hf,vib}/h\nu_{hf,vib}. \tag{8}$$

Here, $\lambda_{hf,vib}$ and $\nu_{hf,vib}$ are the reorganization energy and the frequency of the quantized high-frequency mode. Consequently, the individual rate constant is expressed as

$$k_{NA}^{0\to n} = \frac{2\pi}{\hbar}\frac{1}{\sqrt{4\pi\lambda_s k_B T}}(V_{el}^{0\to n})^2 \exp\left(-\frac{(\Delta G_0^{0\to n} + \lambda_s)^2}{4\lambda_s k_B T}\right). \tag{9}$$

I-3. Effect of Solvation Dynamics. In the previous subsections we have assumed that the solvation process is fast compared to the other dynamics involved in ET, and have ignored the effect of the finite response of solvent polarization relaxation. Since the time scale of solvation dynamics is in the picosecond region for normal liquids, this assumption no longer holds for, at least, ET which occurs within the same time range as, or faster than, solvation dynamics.

A theoretical treatment which considers the finite response of the solvent polarization was initiated by Zusman.[8—10] He solved a Landau–Zener-type problem of ET in terms of the stochastic Liouville equation, in which the quantum mechanical electronic transition between the reactant and the product and the classical diffusional motion in the potential well were explicitly included. Rips and Jortner treated the same problem within the framework of quantum mechanical propagators via path-integral calculations for a two-level system coupled to a dielectric, and gave the following simple equation:[15—18]

$$k_{ET} = k_{NA}/(1+\kappa), \tag{10}$$

where κ is the adiabaticity parameter, expressed as

$$\kappa = \frac{4\pi V_{el}^2 \tau_s}{\hbar \lambda_s}. \tag{11}$$

Equation 10 shows a continuous change of ET from the non-adiabatic limit ($\kappa \ll 1$) to the adiabatic limit ($\kappa \gg 1$) in one expression. As can be seen in Eq. 11, the adiabaticity of ET depends on three ET parameters: the coupling between the two electronic states (V_{el}), the solvent reorganization energy (λ_s), which determines the curvature of the potential well, and the relaxation time in the reaction coordinate (τ_s). In the case of ET, λ_s does not depend on the system very much, whereas V_{el} and τ_s can be significantly altered by changing the solvent, temperature and donor–acceptor combinations. We can therefore expect a wide range of variations of ET from the non-adiabatic to adiabatic limits, depending on the reaction conditions with different ET parameters.

In the adiabatic limit ($\kappa \gg 1$) the rate constant can be recast into the following expression:

$$k_A = \frac{1}{\tau_s}\sqrt{\frac{\lambda_s}{16\pi k_B T}} \exp\left(-\frac{\Delta G^*}{k_B T}\right). \tag{12}$$

This problem is reduced to the Kramers- type treatment,[52] where the reaction is considered to be a potential barrier crossing by stochastic motion on the potential energy surface. Calef and Wolynes applied Kramers theory to ET and obtained a similar expression to Eq. 12.[11] In this case the reaction rate constant is inversely proportional to τ_s, and the reaction is called a solvent-controlled adiabatic reaction. At room temperature $16\pi k_B T = 1.2$ eV, and the value of λ_s is usually smaller than this. Therefore, the maximum of k_A is about $1/\tau_s$ for barrierless ET; τ_s is on the order of picoseconds for non-viscous solvents. Thus, for ultrafast ET occurring in the picosecond time regime, it is expected that the solvent fluctuation can be a rate-limiting step.

Kosower and Huppert examined the excited-state intramolecular electron transfer of arylaminonaphthalene sulphonates in alcohol solutions.[53,54] Intramolecular ET occurs from the arylamino to the naphthalene moieties. They found that the ET rate constant was inversely proportional to the longitudinal relaxation time (τ_L) of the solvent. τ_L is the longitudinal relaxation time calculated from the Debye relaxation time (τ_D),

$$\tau_L = \frac{\varepsilon_\infty}{\varepsilon_0}\tau_D, \tag{13}$$

where ε_∞ and ε_0 are the dielectric constants at the high-frequency limit and static limit, respectively.[55] τ_D is obtained by dielectric measurements. For a simple Debye-type solvent with a single dielectric relaxation time it is shown that τ_s is equal to τ_L.[56] The correlation between the solvent-relaxation times and the intramolecular ET rates has been discussed by various authors.[57—68] Kang et al. studied the charge separation of bianthryl from the locally excited state to the charge-transfer state.[65] They found this activationless ET to be a solvent-controlled adiabatic reaction. A similar adiabatic process was also found for 4-(9-anthryl)-*N*,*N*,-dimethylaniline (ADMA).[65,66] The internal conversion from the S_2 to S_1 states of ADMA was faster than the system response, and the following process for the S_1 state was solvent-controlled. The adiabaticity parameter was actually estimated to be about 80 in common polar solvents ($\lambda_s = 7000$ cm^{-1}, $V_{el} = 350$ cm^{-1}, and $\tau_s = 1$ ps).

Jortner and Bixon incorporated the effect of high-frequency quantized vibrational modes in an ET theory which included the effect of solvation dynamics.[18] The framework of this theory is similar to that of the non-adiabatic case. The overall reaction rate constant is the sum of all the rate constants of the vibrational reaction channels,

$$k_{ET} = \sum_n k_{ET}^{0\to n}, \tag{14}$$

where

$$k_{ET}^{0\to n} = k_{NA}^{0\to n}/(1+\kappa^{0\to n}) \tag{15}$$

and $\kappa^{0\to n}$ is an effective adiabaticity parameter between the ground vibrational state of the reactant and the n-th vibrational state of the product, which is expressed as

$$\kappa^{0\to n} = \frac{4\pi (V_{el}^{0\to n})^2 \tau_s}{\hbar \lambda_s}. \tag{16}$$

Equation 14 can be applied to rather limited cases. The rate-constant expression of Eq. 15 takes into account the finite response of the solvation dynamics by considering the effective adiabaticity parameter. On the other hand, the assumption of Eq. 14, the sum of all the rate constants, already considers that the solvent

response is fast compared to the ET dynamics. Therefore, the Jortner–Bixon model can be reasonably well applied to the case in which the solvation is so fast that the overall reaction rate constant can be approximated by the sum of all the rate constants. If the solvation is slow, the reaction may make a "hole" in the distribution of the reactant at the vibrational channels with fast reaction rates, and, thus, the Jortner–Bixon model no longer holds.

Recently, Jortner and Bixon have developed a new model which considers the solvent-coordinate dependent reaction rate constant and the excitation of intramolecular high-frequency modes.[20] They showed that the effect of solvent relaxation is minor for activationless and inverted-region ET. In this model the problem mentioned above could be safely solved.

I-4. Separation of the Time Scale of the Relaxation in the Reaction Coordinate. (1) Sumi–Marcus Theory: Classical Model for Vibrational Degrees of Freedom. According to Eq. 12, the ET rate constant should not be larger than the inverse of the solvation time. Recent ultrafast experiments have revealed an ET which exceeds the solvation process. Furthermore, some of these ET show non-exponential dynamics. Sumi, Nadler, and Marcus developed an ET theory based on a two-dimensional coordinate model, which predicted fast non-exponential reaction dynamics.[13,14] They partitioned the reaction coordinate into two parts: a vibrational nuclear coordinate (q) and a solvent coordinate (X) as shown in Fig. 3 (Sumi–Marcus theory):[13]

$$G_r(X,q) = \lambda_s X^2 + \lambda_v q^2, \tag{17}$$

$$G_p(X,q) = \lambda_s (X-1)^2 + \lambda_v (q-1)^2 + \Delta G_0. \tag{18}$$

Here, λ_v is the reorganization energy for the classical coordinate (q). In this scheme the relaxation in the nuclear coordinate is assumed to be much faster than that in the solvent coordinate. The quasi particle on the free-energy surface in Fig. 3 moves along X due to thermal fluctuations and a transition from the reactant to the product occurs with some probability at a certain point of X. The population can be expressed by the diffusion-reaction equation,[13]

$$\frac{\partial p(X,t)}{\partial t} = D\frac{\partial}{\partial X}\left[\frac{\partial}{\partial X} + \frac{1}{k_B T}\frac{dV(X)}{dX}\right] p(X,t) - k(X)p(X,t), \tag{19}$$

where D is the solvent polarization diffusion coefficient, $V(X)$ is the free-energy potential of the reactant, and $p(X,t)$ is the classical probability distribution function at X and t. The first term on the right-hand side represents the diffusive motion along the solvent coordinate (X), and the last term represents the reaction along the nuclear coordinate (q).

It is interesting to note that the problem is reduced to a one-dimensional case, as shown in Eq. 19, though the theoretical framework itself is based on the two-dimensional coordinate. This is due to the assumption that relaxation on the vibrational coordinate is much faster than any other dynamics considered here. A similar reaction-diffusion equation was proposed by Bagchi, Fleming, and Oxtoby to include the dynamics of activationless reactions in solution.[69,70]

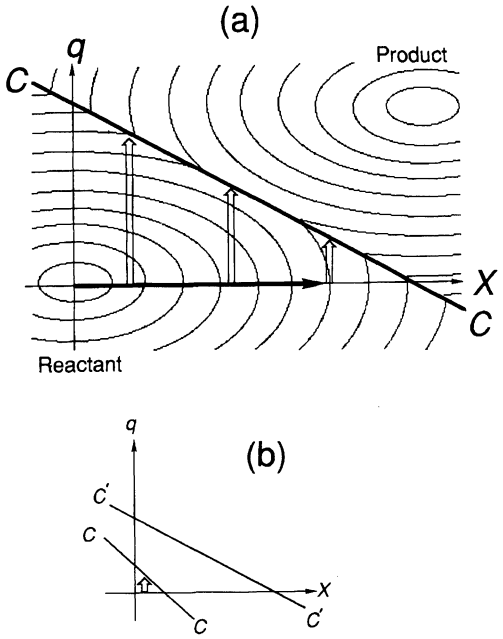

Fig. 3. (a) A two-dimensional expression of the reactant and product free energy surfaces spanned by solvent coordinate X and nuclear coordinate q. A curve C indicates the transition state. (b) A simplified scheme for the location of the transition state with almost no energy barrier (curve C), which gives exponential dynamics or close to exponential dynamics, and with an activation barrier (curve C′) which gives non-exponential dynamics.

In the Sumi–Marcus model, although the vibrational nuclear motion is assumed to be fast compared to other dynamics involved in the reaction, the solvation dynamics are treated as being an overdamped diffusive motion. Thus, although the distribution along X may evolve in time, the distribution along q is always at equilibrium. One can therefore define a rate constant ($k(X)$) at each X with a suitable averaging over the population in the q coordinate,

$$k(X) = \nu_q \exp\left[-\frac{\Delta G^*(X)}{k_B T}\right], \tag{20}$$

where $\Delta G^*(X)$ is the free energy of activation at X, and ν_q is a pre-exponential factor.

If the motion of the solvent is effectively "frozen", the time-dependent survival probability of the reactant state ($P(t)$) can be approximately given by

$$P(t) = \int p(X,0)\exp[-k(X)t]dX. \tag{21}$$

One of the important points of this theory is that the different reaction rate constant ($k(X)$) at each X

changes the distribution of the reactant during the reaction, and gives rise to a non-exponentiality in the reaction kinetics. If the solvent is not frozen, the population dynamics can be described using the diffusion-reaction equation (Eq. 19).

(2) Extended Sumi–Marcus Theory: Classical and Quantum Mechanical Model for Vibrational Degrees of Freedom. The Sumi–Marcus model treats both the solvent and intramolecular modes purely classically; they used the non-adiabatic expression for $k(X)$, which is a single vibronic channel model. However, the actual system should have not only the classical low-frequency modes, but also quantized high-frequency modes, as mentioned in I-2.

Walker et al. extended the Sumi–Marcus model so as to include the effect of high-frequency modes in a similar manner as that developed in the Jortner–Bixon model.[24] In order to take into account of multiple vibronic channels, the solvent-coordinate dependent rate constant ($k(X)$) is expressed as the sum of a contribution from all vibrational states of the product,

$$k(X) = \sum_n k_{\mathrm{NA}}^{0\to n}(X), \tag{22}$$

where

$$k_{\mathrm{NA}}^{0\to n}(X) = \frac{2\pi (V_{\mathrm{el}}^{0\to n})^2}{\hbar\sqrt{4\pi\lambda_{\mathrm{cl,vib}} k_{\mathrm{B}} T}} \exp\left(-\frac{(\Delta G_0^{0\to n}(X) + \lambda_{\mathrm{cl,vib}})^2}{4\lambda_{\mathrm{cl,vib}} k_{\mathrm{B}} T}\right). \tag{23}$$

Here, $\lambda_{\mathrm{cl,vib}}$ is the classical reorganization energy of the low-frequency vibration. In this model Walker et al. divided the classical reorganization into two parts: terms corresponding to the classical vibrations and to solvent reorganization. They experimentally obtained the values of these parameters by spectroscopic means (described later). $\Delta G_0^{0\to n}(X)$, the effective energy gap between the ground vibrational state of the reactant and the n-th vibrational state of the product, is solvent coordinate dependent, as follows:

$$\Delta G_0^{0\to n}(X) = \lambda_{\mathrm{s}} + \Delta G_0 - 2\lambda_{\mathrm{s}} X + nh\nu. \tag{24}$$

Here, it is assumed that the vibrational relaxation of the internal degrees of freedom in the reactant and the product is fast on the ET time scale. In later sections we show several examples of ET which can be rationalized by this extended model.

The original Sumi–Marcus theory was applied to several ET systems to explain a non-exponential feature of the dynamics and/or a reaction rate faster than solvation.[33,60,62,63] Simon and coworkers studied intramolecular ET in the excited states of *N,N*-dimethylaminobenzonitrile (DMABN)[62] and bis[(*N,N*-dialkylamino)phenyl]sulfone[63] in various alcohols over a wide range of temperatures. They found that ET occurred faster than the solvation process, and showed non-exponential behavior. They explained these observations in a qualitative manner using the Sumi–Marcus model. Poellinger et al. observed intramolecular ET of porphyrin-quinone cyclophanes, and found the rate constant to be limited to be on the order of 10^{12} s^{-1}, regardless of the solvent polarity.[68]

Recently, ET reactions much faster than the solvation dynamics were observed. Walker et al. studied ultrafast intramolecular ET in betaines, and analyzed the results in terms of the extended Sumi–Marcus model.[24] Tominaga et al. found a metal–metal charge transfer of mixed-valence compounds which is faster than the diffusive solvation process.[32] Kobayashi et al. studied ultrafast intermolecular ET.[33,34] They found a fluorescence quenching as fast as 100 fs for Nile blue A perchlorate (NB) in *N,N*-dimethylaniline (DMA), and somewhat slower non-exponential fluorescence quenching in aniline (AN).[33] Later, many similar examples were found with oxazines and coumarins.[35—41] They discussed the ET dynamics by considering the contribution of the vibrational degrees of freedom as well as that of the solvent. Most recently, other examples of intermolecular ET have been reported in systems of a benzene-bromine atom charge-transfer complex[71] and of a tetracyanoethylene–hexamethylbenzene system.[72] In a later section we discuss the intramolecular ET studied by Barbara and coworkers as well as intermolecular ET studied by us in detail.

II. Solvation Dynamics

As described in the previous chapter, ET in a solution is often a direct function of the solvent properties. However, it was only recently that the contribution of the dynamical properties of the solvent to the microscopic mechanism of ET has attracted researchers' attention. Reliable information concerning short-time behavior of solvent relaxation is particularly important. There are mainly two different ways to estimate the solvation times. One way uses dielectric dispersion and loss data. The dielectric spectra can be fitted using model functions of the frequency of an applied alternating electric field.[55] From this analysis the characteristic times of dielectric relaxation can be estimated. In order to obtain information concerning the solvation dynamics we must invoke several theoretical models[55,73,74] in order to connect the dielectric data with the dynamical behavior of the solvent polarization. The simplest example is already given in Eq. 13.

The second method is more direct: The energy relaxation of the excited electronic state of a proper probe molecule in a polar solvent is measured by monitoring the dynamic fluorescence Stokes shift of the probe molecule. This method has been extensively used in studies of the solvation process of many different liquids.[64,75] The idea of this experiment is illustrated in Fig. 4. Briefly, when a probe dye molecule immersed in a liquid is photo-excited, the dipole moment of the molecule varies instantaneously. The polarization of the

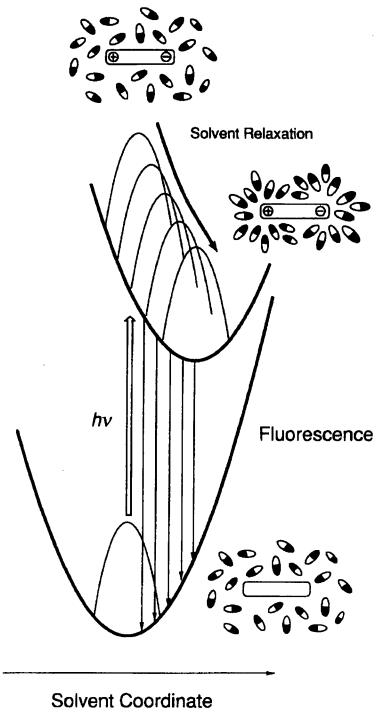

Fig. 4. A schematic drawing showing dynamic fluorescence Stokes shift caused by solvation process on the excited-state free energy surface.

surrounding solvent molecules responds to this change and reorganizes. The energy relaxation of the excited probe is monitored by observing any shift of the fluorescence spectrum. Traditionally, a dynamical feature of the solvent relaxation is discussed in terms of the normalized response function, defined as

$$C(t) = \frac{\nu(t) - \nu(\infty)}{\nu(0) - \nu(\infty)}, \tag{25}$$

where $\nu(t)$, $\nu(\infty)$, and $\nu(0)$ are the fluorescence peak frequencies at times t, ∞, and 0, respectively. For this method, a probe molecule should change its dipole moment upon photo-excitation. Particularly, coumarin C102 (Fig. 5) is one of the probe molecules which is often used for the experiment, since a molecular structure is not expected to change very much due to photo-excitation because of the rigid structure.[76—78] A comprehensive review of solvation dynamics, including developments of theoretical treatments and computer simulations, was recently presented by Maroncelli.[75]

As an example, Fig. 6 shows fluorescence decays of C102 in DMA and AN observed at different wavelengths by a fluorescence-up conversion method using a femtosecond Ti:sapphire laser.[39] Similarly to other solvation experiments,[76—79] there is a fast decay in the shorter wavelength side and a concurrent rise in the longer wavelength side. This implies that the fluorescence spectrum of C102 shifts towards red with time. By reconstructing time-resolved fluorescence spectra using transients at different wavelengths and the static

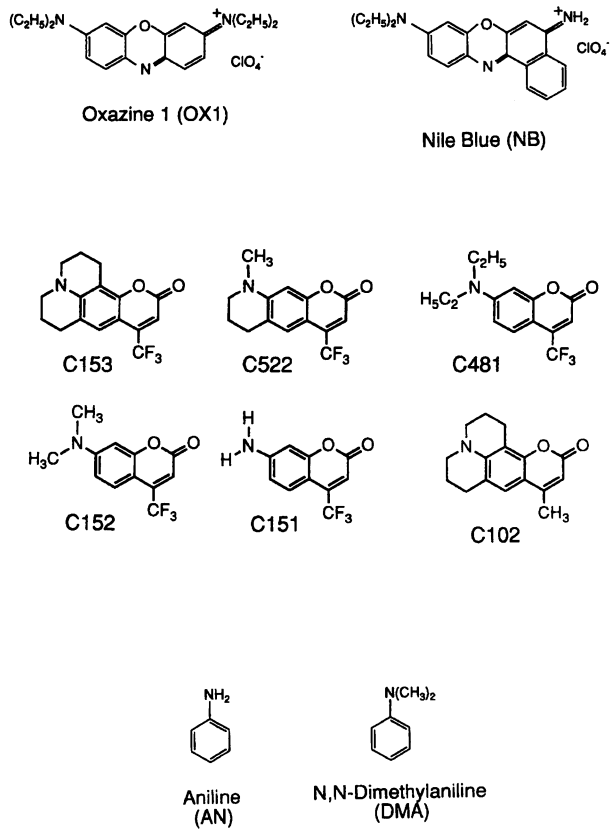

Fig. 5. Molecular structures of dyes, oxazines, and coumarins described in this article. Two solvent molecules aniline (AN) and *N,N*-dimethylaniline (DMA) are also shown.

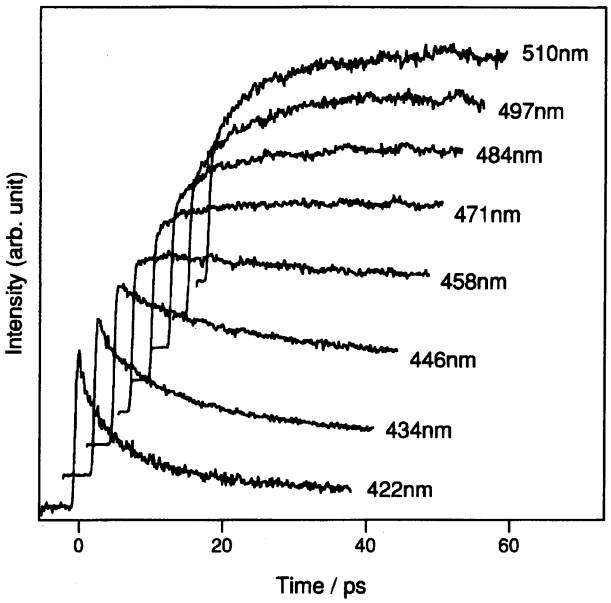

Fig. 6. Fluorescence decays of coumarin 102 (C102) in aniline measured at various wavelengths.

fluorescence spectrum, $C(t)$ can be determined experimentally. $C(t)$ of AN and DMA shows a non-exponential feature and can be fitted well by a bi-exponential

function. The obtained solvent relaxation times are 7.9 ps (19%) and 18.7 ps (81%) for DMA and 1.2 ps (28%) and 17.8 ps (72%) for AN.[80]

Recently, the initial response of the solvation dynamics has attracted much attention. The relaxation of the solvent polarization occurs on a distribution of time scales. These time scales can be roughly separated into faster inertial components on the order of tens of femtoseconds and slower overdamped components on the order of picoseconds or longer, depending on the solvent and temperature. This inertial component, which is due to molecular motion without collisions, was first predicted by computer simulations[81—84] and experimentally observed in acetonitrile.[85] The inertial dynamics are characterized by a Gaussian form of $C(t)$ as well as their fast nature. To distinguish the inertial dynamics from slower, underdamped processes, which are characterized by an exponential form of $C(t)$, we sometimes call the latter "diffusive" processes.

III. Ultrafast Intramolecular Electron Transfer

Recently, a couple of groups have made significant steps towards understanding of the roles of the solvation dynamics and vibrational modes in intramolecular ET in solution.[42,57,58,61,64] Among them, Barbara and coworkers investigated reverse ET after photo-excitation to the charge-transfer band of betaines[24—29] and mixed-valence compounds[30—32] by monitoring the recovery of the ground-state absorption. They analyzed the data using the extended Sumi–Marcus model with solvent and intramolecular parameters obtained by independent spectroscopic experiments, and showed good agreements between the ET rate constants obtained experimentally and the calculated results.

III-1. Temperature and Solvent Dependence of ET; Betaines. Betaines have a charge-separated ground state and a weakly polar first excited state, and are extensively used as an empirical probe for solvent polarity owing to their large change in the dipole moment upon photo-excitation (Scheme 1).[87] Barbara and coworkers measured the reverse ET rate constant (k_{ET}) in various kinds of solvents, from non-polar solvents like benzene to polar solvents like acetonitrile, over a wide range of temperatures. Some of the results are shown in Figs. 7 and 8. Figure 7 illustrates the ET time ($1/k_{ET}$) as a function of the solvation times measured by the fluorescence dynamic Stokes shift method. The ET time shows a bi-phase dependence on the solvation time. In fast relaxing solvents with solvation times (τ_s) less than 3 ps the ET time is approximately proportional to τ_s, but remains almost constant at 2 to 5 ps in slowly relaxing solvents with solvation times greater than 10 ps, even by several orders of magnitude. Figure 8 shows the temperature dependence of k_{ET} from 347 to 228 K in glycerol triacetine (GTA). At 347 and 228 K k_{ET}

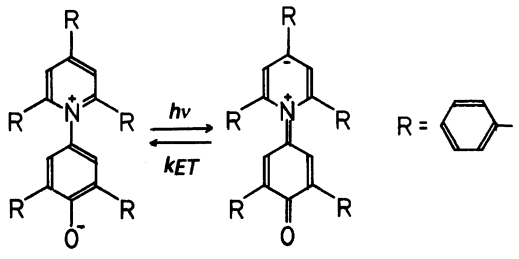

Scheme 1.

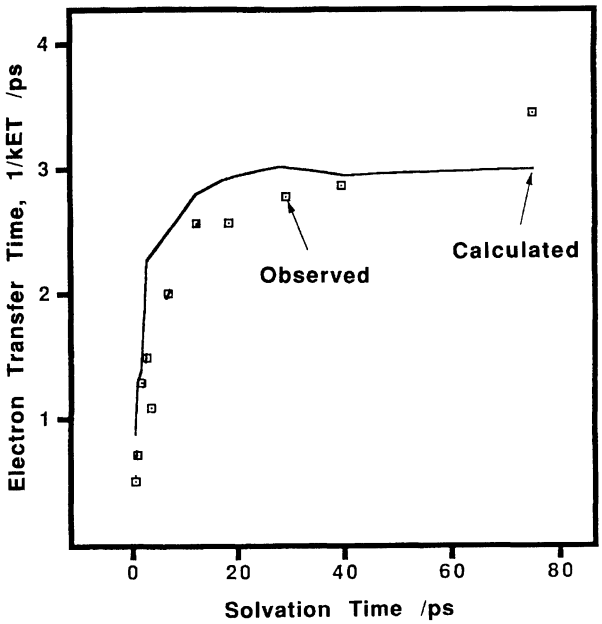

Fig. 7. Symbols; experimentally obtained electron transfer (ET) times, $1/k_{ET}$, for betaine measured by transient absorption technique. Solid curve. ET times predicted by the extended Sumi–Marcus theory.

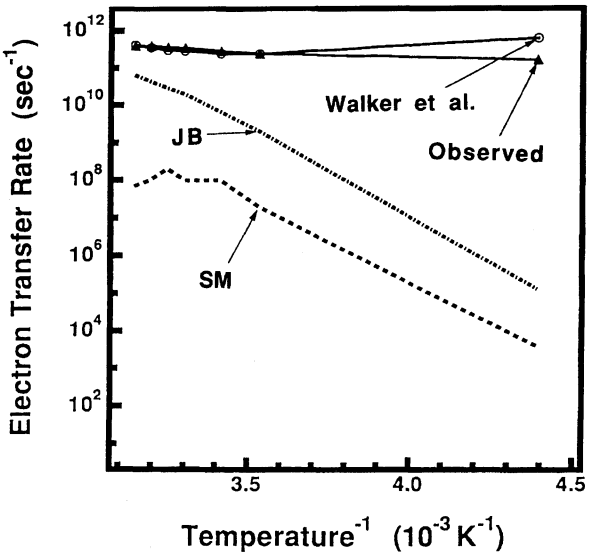

Fig. 8. Arrhenius plot of experimental data and theoretical predictions of electron transfer (ET) times, $1/k_{ET}$, for betaine-30 in glycerol triacetine.

is 0.47×10^{-12} and 0.18×10^{-12} s^{-1}, respectively, and shows a small temperature dependence (Fig. 8).

They explained the variation of k_{ET} within the framework of the extended Sumi–Marcus model. A quantitative picture of the dependence of k_{ET} on the solvation time is as follows. Optical excitation initially prepares a non-equilibrium state on the solvent coordinate with $k(X)$, of which the activation barrier depends on X. In fast relaxing solvents the solvent polarization at first diffuses to a solvent configuration with a relatively low activation barrier, then, the reaction occurs at a very fast rate along the classical vibrational coordinate. Since the rate-determining step is the solvation process, the ET time is almost equal to τ_s. On the other hand, in slowly relaxing solvents the system reacts over the barrier at the initial solvent configuration before solvation occurs. Consequently, the rate is almost independent of τ_s. The temperature dependence of k_{ET} is interpreted in a similar way. Since GTA is a slowly relaxing solvent, even at room temperature the solvation is in a "frozen limit", and the reaction rate is determined by $k(X)$ at the initial solvent configuration. Therefore, the temperature dependence results from the barrier height in the initial distribution after photo-excitation. In the case of betaine-30 in GTA, the activation barrier in the initial distribution is rather low, giving a small dependence of the overall rate constant on the temperature.

In order to obtain the ET parameters used in Eq. 23, they fitted the static absorption spectra to a line-shape model which includes one classical degree of freedom with the reorganization energy (λ_{cl}) and one high-frequency quantal degree of freedom with the reorganization energy ($\lambda_{hf,vib}$) and frequency ($\nu_{hf,vib}$). The form of the line shape is the sum of Gaussian functions with Franck–Condon factors, as follows:

$$I(\nu)=\sum_k \frac{(\lambda_{hf,vib}/\nu_{hf,vib})^{k-1}}{k!} \exp\left[\frac{(\nu-(\lambda_{cl}-\Delta G_0+kh\nu_{hf,vib}))^2}{4\lambda_{cl}k_BT}\right]. \quad (26)$$

They partitioned λ_{cl} into $\lambda_{lf,vib}$ and λ_s by assuming $\lambda_{cl}=\lambda_{lf,vib}$ in a non-polar solvent. As an example, the parameters obtained for betaine-30 in acetonitrile are: $\Delta G_0=-11645$ cm^{-1}, $\lambda_{hf,vib}=1276$ cm^{-1}, $\nu_{hf,vib}=1554$ cm^{-1}, $\lambda_{cl}=3644$ cm^{-1}, $\lambda_{lf,vib}=1223$ cm^{-1}, and $\lambda_s=2221$ cm^{-1}. The electronic coupling (V_{el}) was fixed at 2500 cm^{-1} for all the calculations to reproduce the results in GTA at 298 K.

In Figs. 7 and 8 the calculated results obtained by the extended Sumi–Marcus model are shown. The agreements between the experiments and predictions are excellent, confirming the qualitative picture mentioned above. In Fig. 8 the calculated results obtained by the original Sumi–Marcus and Jortner–Bixon models using the same parameters are also shown. Obviously, the extended model predicts the experimentally observed values much better than the other models. The failure of the original Sumi–Marcus model may be traced to the large barrier along the classical vibrational coordinate for the ET at low temperatures, and the failure of the Jortner–Bixon model may be traced to its dependence on solvent diffusion.

III-2. Extremely Fast ET; Mixed-Valence Compounds. They have also studied reverse ET from the charge-transfer state to the ground state of some mixed-valence compounds in several solvents.[30—32] Mixed-valence compounds have two metal centers in different oxidation states separated by a bridging ligand; the first excited state is the metal-metal charge-transfer (MMCT) state. An example is

$$(NH_3)_5Ru^{III}NCRu^{II}(CN)_5^- \underset{k_{ET}}{\overset{h\nu}{\rightleftharpoons}} (NH_3)_5Ru^{II}NCRu^{III}(CN)_5^-. \quad (27)$$

Because of the solubility of the compound, solvents were limited to be extremely polar ones, such as water, formamide or glycerol. Figure 9 illustrates a couple of transient behaviors of the recovery of the ground-state absorption. For fast-relaxing solvents, such as water or formamide, the ET time ($1/k_{ET}$) is faster than the system response (about 100 fs) and is almost independent of the temperature. In glycerol the ET time is 0.33 ps and 0.74 ps at room temperature and 173 K, respectively. An interesting observation is a solvent isotope effect on the reaction rate; in glycerol, the value of k_{ET}(glycerol)/k_{ET}(glycerol-d_3) is 1.2 at 293 K and 1.5 at 173 K.

The overall ET dynamics of mixed-valence compounds are qualitatively similar to those of betaines. The lack of a strong temperature dependence precludes a simple, thermally activated mechanism for the ET, and suggests that high-frequency vibrational modes of the reactant play a role in promoting the reaction. Another important issue is the role of the solvation dynamics on the ET rates. Since ET is quite fast, and is almost comparable to the inertial-type underdamped solvation dynamics, the effect of the inertial component is not negligible. This is supported by the solvent isotope effect. Since the isotope effect is observed even at cryogenic temperatures, where overdamped diffusive solvent motions should be too slow to be significant, this isotope effect should most likely be ascribed to solvent librational modes.

In order to analyze the ET data using the extended Sumi–Marcus model, they obtained the ET parameters by simulating the MMCT absorption bands using the resonance Raman spectra. They incorporated eight Raman-active modes instead of one high-frequency mode in Eq. 26, and obtained the classical reorganization energy, energy gap, and reorganization energy of each high-frequency mode. A similar band-shape analysis using Raman data was performed by Myers and co-workers on the intermolecular ET systems of hexamethylbenzene and tetracyanoethylene to obtain the

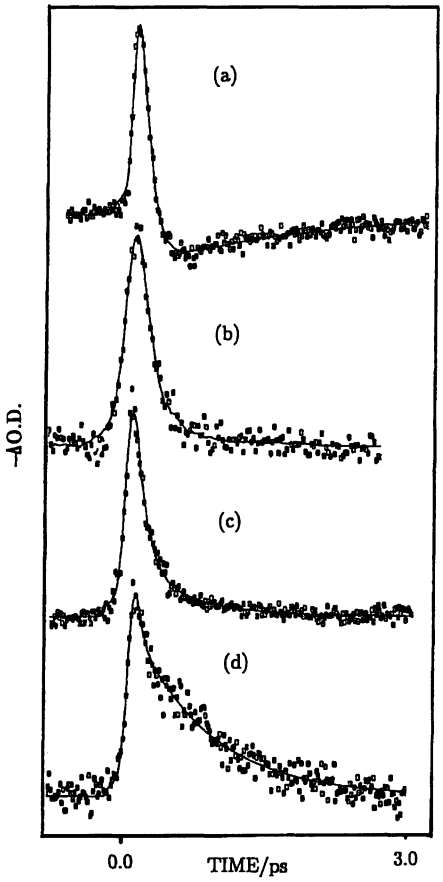

Fig. 9. Change in absorption as a function of time delay between the pump and probe pulses for reaction of Eq. 27 in H_2O at 293 K (a and b), *N*- methylformamide at 293 K (c), and glycerol at 173 K (d). $\lambda_{pump}=\lambda_{probe}=792$ nm for a, c, and d, and $\lambda_{pump}=800$ nm and $\lambda_{probe}=700$ nm for b. A positive signal indicates a bleach. The points are the experimental data, and solid curves show biexponential fits to the data.

ET parameters.[88] An example in the present case is $\lambda_{cl}=3700$ cm^{-1}, $\Delta G_0=-7880$ cm^{-1}, and the total vibrational reorganization energy is 2169 cm^{-1} for the mixed-valence compound in Eq. 27 in D_2O.

In quantitative analyses they used a two-dimensional coordinate system comprising a classical underdamped coordinate ("fast" coordinate) to describe the intramolecular low-frequency modes and the inertial component of solvation and classical overdamped coordinate ("slow" coordinate) to describe the diffusive component of solvation. For the solvent-coordinate dependent rate constant ($k(X)$) they used three different contemporary theories: The non-adiabatic theory as represented by Eq. 23, the Jortner–Bixon theory, and a theory developed by Mukamel and coworkers.[21,22] The second and third ones consider the finite response of the fast coordinate, which is ignored in the first model. The Jortner–Bixon model treats the relaxation on the reaction coordinate as an exponentially decaying process, whereas the theory of Mukamel and coworkers can incorporate any functional form for the time correlation function of this coordinate. Barbara and coworkers chose a Gaussian function for the time-correlation function, which is based on an assumption that the fast coordinate is dominated by the contribution of the inertial solvation dynamics. Since a relative ratio of the underdamped components of the solvation to the overdamped one is unknown, they calculated the reverse ET time ($1/k_{ET}$) as a function of the fraction of the fast component. The results are shown in Fig. 10. Several computer simulations showed that the fraction of the fast component is 50 to 80% for H_2O.[75,83,84] The Jortner–Bixon and Mukamel and coworkers' models can satisfactorily explain various observations, including the temperature dependence, isotope effect, and difference of different mixed-valence compounds. They concluded that the strong vibronic coupling between the reactant and product and the inertial component of nuclear motion play important roles in the ET dynamics of mixed-valence compounds.

IV. Intermolecular Electron Transfer

During several recent years we studied *intermolecular* ET between excited dye molecules and electron-donating solvents and found that some of these ET are much faster than the solvation dynamics and undergo non-exponential kinetics.[33—41] As dye molecules we chose oxazine 1 (OX1), Nile blue (NB), and coumarins with different structures; as solvents we chose aniline and *N*,*N*-dimethylaniline (see Fig. 5 for the structures of these molecules).

IV-1. Intermolecular Electron-Transfer Dynamics and the Temperature Dependence. (1)

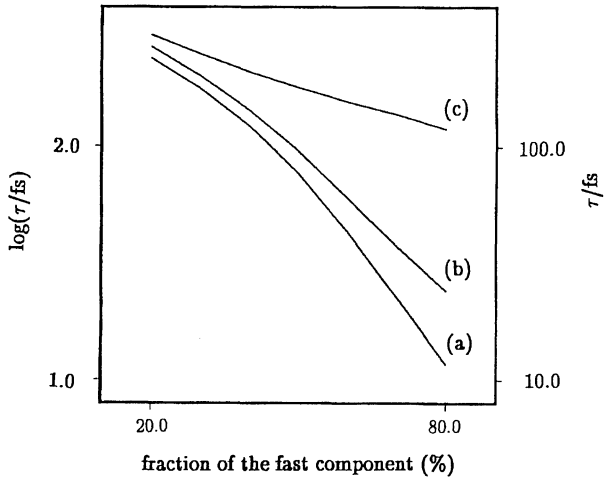

Fig. 10. Theoretically predicted ET times, $1/k_{ET}$, for reaction of Eq. 27 as a function of the fraction of the fast component. (a), (b), and (c) denote the predictions by non-adiabatic, Jortner–Bixon's, and Mukamel and co-workers' theories, respectively, for the reaction along the fast coordinate.

Summary of Experimental Results. The dyes used in the present work were strong fluorescent substances, which are often used as laser dyes. However, when they are dissolved in the electron-donating solvents, the fluorescence is severely quenched. The fluorescence intensity of coumarins in DMA is more than 1000-times weaker than that in ordinary solvents (Fig. 11). Using a sub-picosecond transient absorption technique[35,39] it was concluded with cationic dyes (NB and OX1) that fluorescence quenching was due to intermolecular ET from the solvent molecule to the excited dye; the reaction products, namely, neutral radicals of the dye and solvent cation, were identified in the transient absorption spectra.

The fluorescence decays of OX1 in the donor solvents are shown in Fig. 12. The decay of OX1 in DMA is almost single exponential with a time constant of 280 fs, though OX1 in AN gives a non-exponential decay. A tentative fitting was made by a triple exponential function for the decay in AN, the fitting parameters being 460 fs (40%), 1.6 ps (57%), and 18 ps (3%) at 285 K.[36]

In the present system several interesting features were observed: (1) ET is much faster than the diffusive solvation process. Especially in DMA, ET seems to occur approximately 50-times faster than the solvation process for the fastest dyes. (2) Although OX1 in DMA shows an extremely fast single-exponential ET, in AN it shows a somewhat slower non-exponential ET. (3) Back ET occurs successively from the neutral radical of

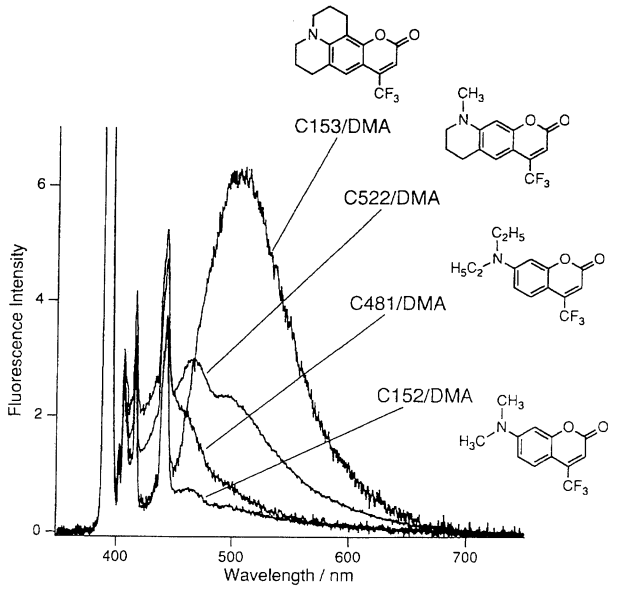

Fig. 11. Steady-state fluorescence spectra of selected coumarins in DMA. The fluoresence is so weak that its in tensity is comparable to the Raman bands of solvent (structured spectra). Electron transfer is faster in the order of C153<C522<C481<Cl52. The faster dyes show bluer-shifted fluorescence (see the Section IV-2 (2)).

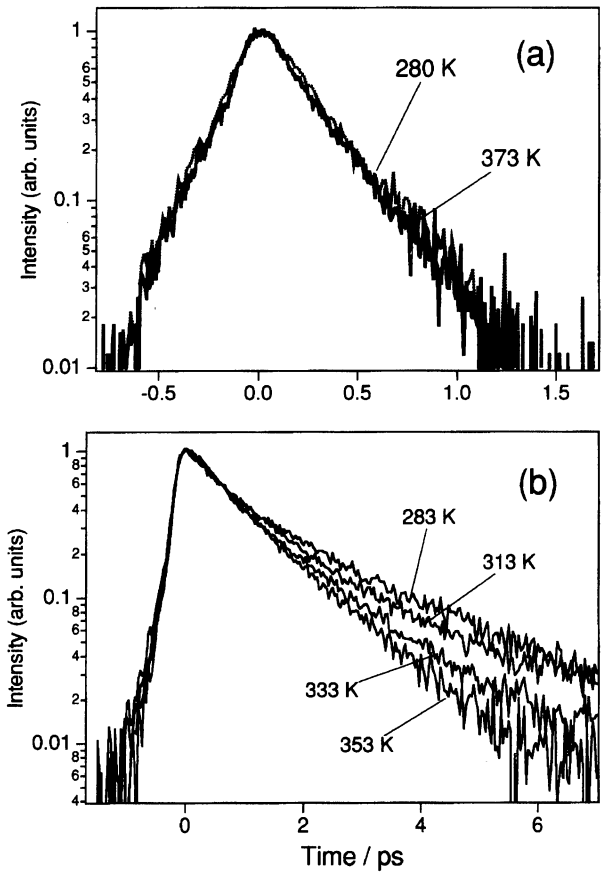

Fig. 12. Fluorescence decays of OX1 (a) in DMA and (b) in AN. The former shows an exponential decay (280 fs) with no temperature dependence between 280 and 373 K. The latter shows non-exponential decay with a clear temperature dependence at slower decay components.

the dye to the solvent cation, and the system returns to the ground state again. The lifetime of the radical ion pair of NB and DMA was 4.0 ps,[35] and that of OX1 and DMA was 4.7 ps.[39]

The temperature dependence of the fluorescence decay of OX1 in the anilines is also shown in Fig. 12.[40] The ultrafast single-exponential decay (280 fs) of OX1 in DMA does not show a temperature dependence from 280 to 373 K. In AN, however, a clear temperature dependence is observed in its non-exponential decay. As the temperature increases from 283 K to 353 K, the decay becomes faster. Although the fastest component (ca. 430 fs) of the triple exponential fittings does not show any temperature dependence, the second component (1.6 ps at 280 K) shows a dependence, which gives an activation energy of 350 cm^{-1}.

(2) ET Analysis Based on the Extended Sumi–Marcus Model. We now analyze the ET dynamics of the present systems while keeping in mind the various characteristics of the experimental results described above. We mainly invoke the extended Sumi–Marcus model to rationalize all of the experimen-

tal results. A qualitative picture of the reaction dynamics is as follows. The electronic states associated with the present intermolecular ET are the S_1 state and the charge-transfer (CT) state. On the other hand, those for the intramolecular ET of the betaines and mixed-valence compounds are the S_0 and photo-induced CT. Since OX1 does not change its electric dipole moment upon photo-excitation very much, it is reasonably assumed that the initially prepared state in the reactant (the S_1 state) is almost identical to that thermally equilibrated in the reactant (see Fig. 3(a)). The reaction takes place along the q coordinate; if the ET dynamics are comparable to or slower than the solvation dynamics, a reorganization of the solvent configuration occurs simultaneously.

We attribute the difference between the ET dynamics in AN and DMA, namely the difference in the reaction rate and exponentiality of the kinetics, to a difference in the energy gap (ΔG_0). Since there is almost no activation barrier in the case of OX1 in DMA, the product surface can be considered to intersect with the reactant surface very close to the origin of the reactant surface where the initial state is prepared (Fig. 3(b)). In this case the reactant can overcome the reaction barrier very rapidly, regardless of the slope of curve C, and a single-exponential kinetic is expected. If the value of $-\Delta G_0$ is larger, which corresponds to the AN case, curve C is far away from the origin, and thus slower and non-exponential ET dynamics with an activation barrier are anticipated. In the present system ET in AN is in the "normal region", and in DMA on the top of the "bell shape" (Fig. 1).

The difference in the energy gap results from the difference in the ionization potential. The ionization potential of liquid DMA was calculated to be 0.17 eV smaller than that of AN by invoking gaseous ionization potentials (I_{vap}) and the following formula:[89]

$$\Delta I_{cond} = I_{vap}^{AN} - I_{vap}^{DMA} - \left(1 - \frac{1}{\varepsilon_{AN}}\right)\frac{e^2}{2r_{AN}} + \left(1 - \frac{1}{\varepsilon_{DMA}}\right)\frac{e^2}{2r_{DMA}}, \quad (28)$$

where ε is the dielectric constant, e the electronic charge, and r the radius of the charged solvent molecule. This difference causes a difference in the free-energy gap for the reaction, and, thereby, the free-energy barrier for the reaction. This explains the faster reaction in DMA as well as the observed temperature dependence if the reaction in DMA is barrierless and the reaction in AN has a small activation energy.

To see the validity of this assumption, we have performed simulations using the extended Sumi–Marcus model. The essential point of the simulation is whether the experimental results can be reproduced by changing only ΔG_0 by 0.17 eV with other parameters fixed between the AN and DMA cases. Since the parameters necessary for the calculations should be determined in a somewhat arbitrary fashion in this case, the purpose of the simulation is not to obtain the ET parameters precisely, but to explain the ET dynamics semi-quantitatively with physically reasonable values for the parameters.

In the OX1 case neither the fluorescence nor the absorption of the charge-transfer state has been observed, making the spectroscopic determination of the ET parameters very difficult. This is in contrast to the intramolecular case in which the resonance Raman spectroscopic data are available to obtain the parameters by fitting the photo-induced charge-transfer absorption bands. We determined the parameters so as to reproduce the experimental results reasonably well. We used 0.062 eV for the solvent reorganization energy (λ_s), 0.186 eV for the reorganization energy of the low-frequency mode (λ_v), and 0.0105 eV for the electronic matrix element (V_{el}). The time-dependent diffusion coefficient ($D(t)$) was estimated by

$$D(t) = -\frac{k_B T}{2\lambda_s}\frac{1}{\Delta(t)}\frac{d\Delta(t)}{dt}, \quad (29)$$

where

$$\Delta(t) = a_1 \exp(-t/\tau_1) + a_2 \exp(-t/\tau_2). \quad (30)$$

Here, τ_1 is the first and τ_2 is the second solvation time, and $a_1+a_2=1$. For these parameters we used those obtained by the dynamic Stokes shift experiment.

The results of the simulations are given in Fig. 13. The total population of the reactant ($P(t)$), the integral of $p(X,t)$ over X, is plotted as a function of time on the logarithmic scale. The energy gap ($-\Delta G_0$) is 0.248 eV for Fig. 13(a) and 0.078 eV for Fig. 13(b). Figure 13(a) corresponds to the ET of OX1 in DMA, where there is no activation barrier. The free-energy surfaces of the reactant and product intersect at the bottom of the reactant surface. Such a situation occurs when $-\Delta G_0=\lambda_v+\lambda_s=0.248$ eV. The simulated reaction kinetics shown in Fig. 13(a) is almost exponential, which coincides with the experimental result of OX1 in DMA shown in Fig. 12(a). Figure 13(b) corresponds to the ET of OX1 in AN, which gives non-exponential dynamics; the reaction becomes faster as the temperature increases. The major difference in the reaction dynamics is a difference in $-\Delta G_0$ of 0.17 eV. In the simulation, the first component shows almost no activation barrier, whereas the second component has an activation barrier of 270 cm^{-1}. This value is in good agreement with the experimental result (350 cm^{-1}).

In the case of Fig. 13(a), it is notable that the reaction becomes *slower* at higher temperature. This is because the population in the reactant well is distributed over a wider region of the solvent coordinate at higher temperatures, and because the reaction takes place fastest near to the bottom of the well due to the coordinate-dependent rate constant ($k(X)$). An increase in the temperature spreads the distribution to a region where the

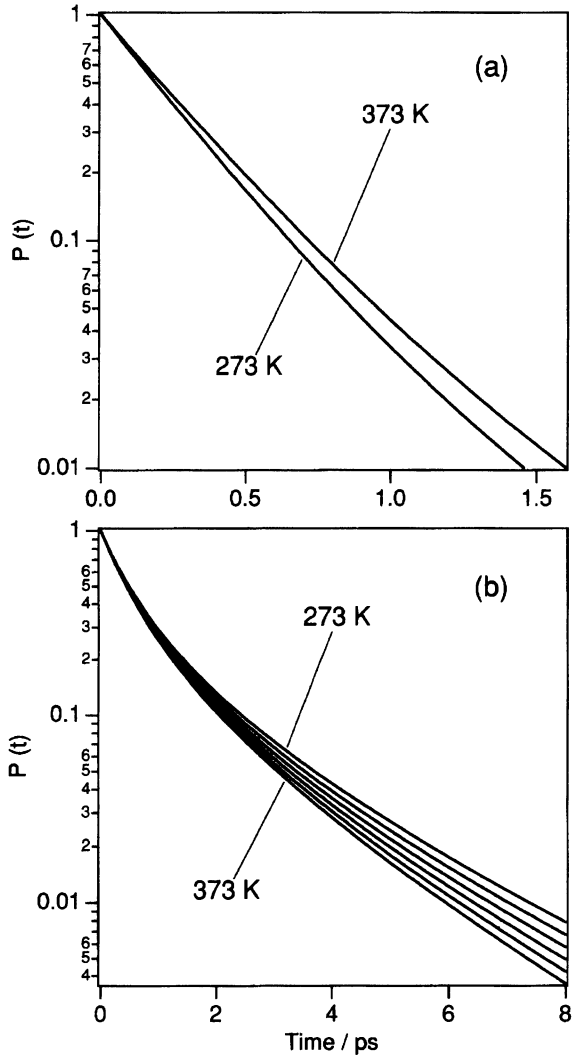

Fig. 13. Simulation of temperature dependence of fluorescence decays using the extended Sumi–Marcus model. (a) $-\Delta G_0$=0.248 eV, T=273 and 373 K. (b) $-\Delta G_0$=0.0781 eV, T=273, 293, 313, 353, and 373 K.

reaction occurs less-effectively. However, no significant temperature dependence was observed for OX1 in DMA within the experimental error. Presumably, this was due to the limited signal-to-noise ratio of the signal as well as the arbitrariness of the ET parameters used in the simulation.

In the above analysis it is not necessarily needed to invoke the extended Sumi–Marcus theory to explain the experiments; the original Sumi–Marcus model, in which the high-frequency mode is not considered, can rationalize the experimental results reasonably well. This is because the free-energy surfaces are not in the inverted region and the initially prepared state in the reactant surface is close to that thermally equilibrated in the reactant. However, the high-frequency vibrational modes play an important role in the ET of coumarins in the electron-donating solvents, which is discussed in the next section.

IV-2. Substituent Effects on Intermolecular Electron Transfer. Similar types of the experiments have been performed on various coumarin dyes with different structures in AN and DMA, and the substituent effects on ultrafast intermolecular ET have been systematically examined.[37,41]

(1) Time-Resolved Fluorescence of Ultrafast Reacting Systems. We focus our attention on two positions of coumarins, namely the 4- and 7-positions. Some examples are shown in Fig. 5. The fluorescence decays of 4-CF_3 coumarins, which have a CF_3 group in the 4-position, are shown in Fig. 14.[37] The results of fittings are shown in Table 1. Regarding these series of measurements, there have been several interesting observations: (1) Most of the ET of 4-CF_3 coumarins are faster than the diffusive solvation process. (2) Most of them show non-exponential fluorescence decay. The results of the analysis shown in Table 1 were tentatively obtained with a double-exponential function, except for the single-exponential function with a time constant of 210 fs for the fastest system of C151 in DMA. (3) For

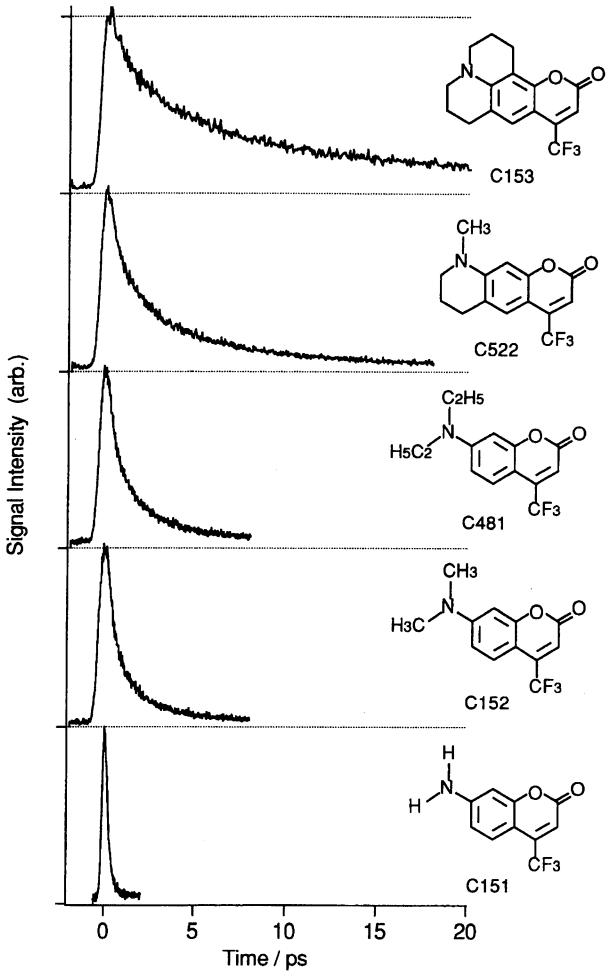

Fig. 14. Fluorescence quenching of 4-CF_3 coumarins in DMA excited at 395 nm and observed at 470 nm for C153, C522, C481, and C152 and 446 nm for C151. Concentrations are 2×10^{-3} M.

Table 1. Absorption λ_{abs} and Fluorescence λ_{flu} Maximum, Stokes Shift $\Delta\nu$, Reduction Potential $E_{red}(dye^{0/-})$, Relative Energy Gap ΔG_{rel}, and Fluorescence Lifetimes τ_{ET} of 4-CF_3 Coumarins

Fluorescence decays were measured at 470 and 510 nm for C153, C522, C481, and C152 in DMA and AN, respectively, and at 430 and 446 nm for C151 in DMA and AN, respectively. The lifetimes for C153 in AN were obtained by global analysis.

	in DMA							in AN						
	λ_{abs}	λ_{flu}	$\Delta\nu$	$E_{red}(dye^{0/-})$[a]	ΔG_{rel}[b]	τ_{ET}[c]		λ_{abs}	λ_{flu}	$\Delta\nu$	$E_{red}(dye^{0/-})$[a]	ΔG_{rel}[b]	τ_{ET}[c]	
	nm	nm	cm^{-1}	V	eV	ps		nm	nm	cm^{-1}	V	eV	ps	
C153	416	504	4200	−2.4	0.00	3.1	{67%}	435	526	3990	−1.76	0.17	11.7	{37%}
						19.4	{33%}						83.8	{63%}
						[8.5]							[57.3]	
C522	408	463	2910	−2.2	−0.26	0.8	{69%}	422	512	4170	−1.72	0.04	10.1	{39%}
						4.0	{31%}						34.4	{61%}
						[1.8]							[25]	
C481	400	448	2680	−2.2	−0.32	0.57	{80%}	413	505	4410	−1.69	−0.05	4.1	{37%}
						2.9	{20%}						15.2	{63%}
						[1.0]							[11]	
C152	397	446	2770	−2.1	−0.44	0.46	{89%}	408	504	4670	−1.68	−0.10	3.7	{41%}
						2.7	{11%}						12.4	{59%}
						[0.71]							[8.8]	
C151	370	410	2630	−2.1	−0.67	0.21	{100%}	376	450	4370	−1.75	−0.29	0.59	{50%}
													1.9	{50%}
													[1.2]	

a) Reduction (peak) potentials from irreversible waves. b) Relative values of energy gap. C153 in DMA is fixed to 0 eV. c) Values in [ ] are the average lifetimes; $\langle\tau\rangle = A_1\tau_1 + A_2\tau_2$.

fast reactions, the lifetimes in DMA are shorter than those of the same coumarins in AN. (4) The reaction rate constant drastically depends on the substituent groups of the coumarin. For substituents in the 4-position, the ET rate increases in the order $-CH_3$ < $-H$ < $-CF_3$. When an alkyl chain in the 7-amino group is extended, the reaction becomes slower, and when it forms a hexagonal alkyl ring with the benzene moiety, the reaction becomes slowest. For the 7-amino group, the reaction rates increase in the following order:

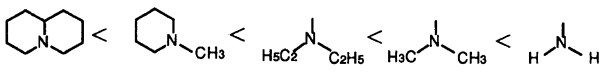

These effects of substitution can be discussed from two aspects: It can change (1) the vibrational mode of coumarin and (2) the free-energy difference of the reactant and product. The substituent effects on ET have been discussed concerning many systems; one of the representative molecules is *N*,*N*-dimethylbenzonitrile (DMABN),[90—92] where the role of the rotational motion of the amino group in ET is a major subject. In the present system, extending the alkyl chain on the 7-amino group and forming a hexagonal alkyl ring may restrict the flexibility of the 7-amino group. Some vibrational modes of the 7-amino group may be involved in the reaction.

We mainly attribute the substituent effects to the difference in the energy gap, and perform a simulation based on the extended Sumi–Marcus model by changing the energy gap while keeping the other ET parameters fixed, similarly to the OX1 case. The way to estimate the parameters and to perform the simulation is almost the same as that of the OX1 case. Although we do not go into details concerning the calculated results in this article, the simulation can reproduce the experimental trend of the reaction rate as a function of the energy gap quite well.[41]

A qualitative picture of the ET dynamics is shown in Fig. 15. Usually, since coumarins change their electric dipole moments drastically upon photo-excitation, the initially prepared state in the reactant is away from the thermally equilibrated one in the S_1 state. The fate of the reactant state is either to perform solvation on the solvent coordinate or to react along the low-frequency vibrational coordinate, depending on the ET rate. We can expect competition between the reaction dynamics and the solvation process if both processes occur on the same time scale. In the case of fast reacting systems, the initially prepared state in the solvent coordinate is close to or in the region where the effectively reacting vibrational channels are located; a reaction quickly takes place through these reaction channels without solvation. By increasing $-\Delta G_0$, the initial population in the reactant potential well is away from the effective vibrational channels, and should be reacted through less-effective channels or perform solvation to reach more effective channels (see Fig. 15). In this case the reaction occurs relatively slowly compared to the case of a small $-\Delta G_0$.

(2) Steady-State Fluorescence of an Ultrafast Reacting System. The competitive dynamics are reflected in the steady-state fluorescence spectra. If a reaction occurs much faster than the solvation proc-

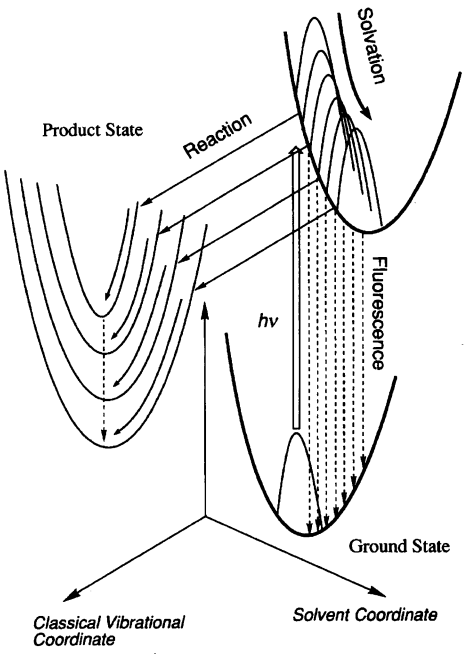

Fig. 15. A conceptual drawing of electron transfer in competition with solvation in the excited state. The solvation occurs on the solvent coordinate and the reaction occurs on the classical low frequency coordinate to the reactant surface with high frequency vibrational levels.

ess, excited molecules only have a chance to fluoresce from the non-equilibrium state before solvent relaxation. This effect can be called either "chemical timing" or "fluorescence gating". The chemical timing has been observed in the fluorescence spectrum of *p*-difluorobenzene in the gas phase using high-pressure oxygen as a quencher, where two competitive processes are intramolecular vibrational redistribution and quenching of the S_1 state by oxygen.[93]

The Stokes shift obtained from the peaks of the absorption and fluorescence spectra is larger than 4000 cm^{-1} for most of these dyes. A slowly reacting dye (C153) in DMA, which has a lifetime close to the solvation time (Table 1 in the section IV), has a Stokes shift of 4200 cm^{-1}. However, for fast reacting dyes, it becomes smaller than 3000 cm^{-1}. The steady-state fluorescence spectra of reacting molecules are shown in Fig. 11. A faster dye (C522) gives a Stokes shift of 2910 cm^{-1}. The fastest dye (C151) in DMA gives only 2630 cm^{-1}. As the rate constant of ET increases, the amount of the fluorescence Stokes shift decreases, as shown in Fig. 11. This is the first example of chemical timing in the condensed phase.

This systematic alteration of the ET rate constant resembles the situation of betaine; in both cases competition between the solvation dynamics and the reaction through the vibrational channels is observed. In the case of betaine the systematic change in the rate constant is caused by a change in the solvation time, whereas the difference in the energy gap is a major factor which alters the ET rate in the coumarin case.

V. Summary

We have overviewed recent theoretical and experimental progress for ET in solution, while especially focusing on the ET which occurs much faster than the solvation dynamics. The dynamical roles of nuclear motions, namely the solvation process and the intramolecular vibration, in ET are of special interest in this article. We have demonstrated that the two-dimensional model, in which the time scales of solvation and the vibrational relaxation are explicitly separated, can explain the ET, which is characterized by its fast rate and non-exponentiality in the kinetics. The extended Sumi–Marcus model, which includes the effect of high-frequency vibrational modes, is necessary to rationalize ET in cases (1) where the reaction is in the inverted region or (2) where the initially photo-prepared state in the reactant is away from that thermally equilibrated in the reactant. In the case of (2), competitive processes between the solvation and reaction have been observed in the transient absorption, time-resolved fluorescence, and steady-state fluorescence spectra.

The author wishes to thank all of the participants of the work presented here. YN wishes to thank the Japan Society for Promotion of Science for the fellowship. KT thanks Professor Paul F. Barbara for his continuous encouragement and helpful discussions. This work was in part supported by the Grant-in Aid for Scientific Research of New Program No. 06NP0301 from the Ministry of Education, Science and Culture.

References

1) R. A. Marcus, *J. Chem. Phys.*, **24**, 966 (1956).
2) R. A. Marcus, *Discuss. Faraday Soc.*, **29**, 21 (1960).
3) R. A. Marcus and N. Sutin, *Biochim. Biophys. Acta*, **811**, 265 (1985).
4) M. D. Newton and N. Sutin, *Annu. Rev. Phys. Chem.*, **35**, 437 (1984).
5) V. G. Levich and R. R. Dogonadze, *Dokl. Acad. Nauk SSSR*, **124**, 123 (1959), (*Proc. Acad. Sci. Phys. Chem. Sect.*, **124**, 9).
6) V. G. Levich, *Adv. Electrochem. Electrochem. Eng.*, **4**, 249 (1966).
7) J. Jortner, *J. Chem. Phys.*, **64**, 4860 (1976).
8) L. D. Zusman, *Chem. Phys.*, **49**, 295 (1980).
9) L. D. Zusman, *Chem. Phys.*, **80**, 29 (1983).
10) L. D. Zusman, *Chem. Phys.*, **119**, 51 (1988).
11) D. F. Calef and P. G. Wolynes, *J. Phys. Chem.*, **87**, 3387 (1983).
12) J. T. Hynes, *J. Phys. Chem.*, **90**, 3701 (1986).
13) H. Sumi and R. A. Marcus, *J. Chem. Phys.*, **84**, 4894 (1986).
14) W. Nadler and R. A. Marcus, *J. Chem. Phys.*, **86**, 3906 (1987).
15) I. Rips and J. Jortner, *J. Chem. Phys.*, **87**, 2090 (1987).

16) I. Rips and J. Jortner, *J. Chem. Phys.*, **87**, 6513 (1987).
17) I. Rips and J. Jortner, *J. Chem. Phys.*, **88**, 818 (1988).
18) J. Jortner and M. Bixon, *J. Chem. Phys.*, **88**, 167 (1988).
19) I. Rips, J. Klafter, and J. Jortner, *J. Chem. Phys.*, **94**, 8557 (1990).
20) M. Bixon and J. Jortner, *Chem. Phys.*, **176**, 467 (1993).
21) M. Sparpaglione and S. Mukamel, *J. Chem. Phys.*, **88**, 3265 (1988).
22) Y. J. Yan, M. Sparpaglione, and S. Mukamel, *J. Phys. Chem.*, **92**, 4842 (1988).
23) B. B. Smith, A. Sataib, and J. T. Hynes, *Chem. Phys.*, **176**, 521 (1993).
24) G. C. Walker, E. Akesson, A. E. Johnson, N. E. Levinger, and P. F. Barbara, *J. Phys. Chem.*, **96**, 3728 (1992).
25) E. Akesson, G. C. Walker, and P. F. Barbara, *J. Chem. Phys.*, **95**, 4188 (1991).
26) E. Akkeson, A. E. Johnson, N. E. Levinger, G. C. Walker, T. P. DuBruil, and P. F. Barbara, *J. Chem. Phys.*, **96**, 7859 (1992).
27) N. E. Levinger, A. E. Johnson, G. C. Walker, and P. F. Barbara, *Chem. Phys. Lett.*, **196**, 159 (1992).
28) A. E. Johnson, N. E. Levinger, D. A. V. Kliner, K. Tominaga, and P. F. Barbara, *Pure Appl. Chem.*, **64**, 1219 (1992).
29) A. E. Johnson, N. E. Levinger, W. Jarzeba, R. E. Schlief, D. A. V. Kliner, and P. F. Barbara, *Chem. Phys.*, **176**, 555 (1993).
30) G. C. Walker, P. F. Barbara, S. K. Doorn, Y. Dong, and J. T. Hupp, *J. Phys. Chem.*, **95**, 5712 (1991).
31) D. A. V. Kliner, K. Tominaga, G. C. Walker, and P. F. Barbara, *J. Am. Chem. Soc.*, **114**, 8323 (1992).
32) K. Tominaga, D. A. V. Kliner, A. E. Johnson, N. E. Levinger, and P. F. Barbara, *J. Chem. Phys.*, **98**, 1228 (1993).
33) T. Kobayashi, Y. Takagi, H. Kandori, K. Kemnitz, and K. Yoshihara, *Chem. Phys. Lett.*, **180**, 416 (1991).
34) K. Kemnitz and K. Yoshihara, *Chem. Lett.*, **1991**, 645.
35) H. Kandori, K. Kemnitz, and K. Yoshihara, *J. Phys. Chem.*, **96**, 8042 (1992).
36) A. P. Yartsev, Y. Nagasawa, A. Douhal, and K. Yoshihara, *Chem. Phys. Lett.*, **207**, 546 (1993).
37) Y. Nagasawa, A. P. Yartsev, K. Tominaga, A. E. Johnson, and K. Yoshihara, *J. Am. Chem. Soc.*, **115**, 7922 (1993).
38) K. Yoshihara, A. P. Yartsev, Y. Nagasawa, A. Douhal, and K. Kemnitz, *Pure Appl. Chem.*, **65**, 1671 (1993).
39) K. Yoshihara, Y. Nagasawa, A. P. Yartsev, S. Kumazaki, H. Kandori, A. E. Johnson, and K. Tominaga, *J. Photochem. Photobiol. A*, **80**, 169 (1994).
40) Y. Nagasawa, A. P. Yartsev, K. Tominaga, A. E. Johnson, and K. Yoshihara, *J. Chem. Phys.*, **101**, 5717 (1994).
41) Y. Nagasawa, A. P. Yartsev, K. Tominaga, P. B. Bisht, A. E. Johnson, and K. Yoshihara, *J. Phys. Chem.*, **99**, 653 (1995).
42) H. Heitele, *Angew. Chem., Int. Ed. Engl.*, **32**, 359 (1993).
43) J. R. Miller, L. T. Calcaterra, and G. L. Closs, *J. Am. Chem. Soc.*, **106**, 3047 (1984).
44) G. L. Closs and J. R. Miller, *Science*, **240**, 440 (1988).
45) K. Kemnitz, N. Nakashima, and K. Yoshihara, *J. Phys. Chem.*, **92**, 3915 (1988).
46) J. C. Moser and M. Gratzel, *Chem. Phys.*, **176**, 493 (1993).
47) J. R. Miller, J. V. Beitz, and R. K. Huddleston, *J. Am. Chem. Soc.*, **106**, 5057 (1984).
48) N. Mataga, T. Asahi, Y. Kanda, T. Okada, and T. Kakitani, *Chem. Phys. Lett.*, **127**, 249 (1988).
49) T. Asahi and N. Mataga, *J. Phys. Chem.*, **93**, 6575 (1992).
50) I. R. Gould, R. H. Young, R. E. Moody, and S. Farid, *J. Chem. Phys.*, **95**, 2068 (1991).
51) W. -S. Chung, N. J. Turro, I. R. Gould, and S. Farid, *J. Phys. Chem.*, **95**, 7752 (1991).
52) H. A. Kramers, *Physica*, **7**, 284 (1940).
53) E. M. Kosower and D. Huppert, *Chem. Phys. Lett.*, **96**, 433 (1983).
54) E. M. Kosower and D. Huppert, *Annu. Rev. Phys. Chem.*, **37**, 127 (1986).
55) H. Fröhlich, "Theory of Dielectrics," Oxford Press, London (1949).
56) B. Bagchi, D. W. Oxtoby, and G. R. Fleming, *Chem. Phys.*, **86**, 257 (1984).
57) M. Maroncelli, J. MacInnis, and G. R. Fleming, *Science*, **243**, 1674 (1989).
58) M. J. Weaver and G. E. McManis, III, *Acc. Chem. Res.*, **23**, 294 (1990).
59) G. E. McManis and M. J. Weaver, *J. Chem. Phys.*, **90**, 912 (1989).
60) D. K. Phelps and M. J. Weaver, *J. Phys. Chem.*, **96**, 7187 (1992).
61) J. D. Simon, *Acc. Chem. Res.*, **21**, 128 (1988).
62) S. -G. Su and J. D. Simon, *J. Chem. Phys.*, **89**, 908 (1988).
63) J. D. Simon and R. Doolen, *J. Am. Chem. Soc.*, **114**, 4861 (1992).
64) P. F. Barbara and W. Jarzeba, *Adv. Photochem.*, **15**, 1 (1990).
65) T. J. Kang, W. Jarzeba, P. F. Barbara, and T. Fonseca, *Chem. Phys.*, **149**, 81 (1990).
66) K. Tominaga, G. C. Walker, W. Jarzeba, and P. F. Barbara, *J. Phys. Chem.*, **95**, 10475 (1991).
67) K. Tominaga, G. C. Walker, T. J. Kang, P. F. Barbara, and T. Fonseca, *J. Phys. Chem.*, **95**, 10485 (1991).
68) F. Poellinger, H. Heitele, M. E. Michel-Beyerle, C. Anders, M. Futscher, and H. A. Staab, *Chem. Phys. Lett.*, **198**, 645 (1992).
69) B. Bagchi, G. R. Fleming, and D. W. Oxtoby, *J. Chem. Phys.*, **78**, 7375 (1983).
70) B. Bagchi and G. R. Fleming, *J. Phys. Chem.*, **94**, 9 (1990).
71) R. E. Schlief, W. Jarzeba, K. A. M. Thakur, J. C. Alfano, A. E. Johnson, and P. F. Barbara, *J. Mol. Liq.*, **61**, 201 (1994).
72) K. Wynne, C. Galli, and R. M. Hochstrasser, *J. Chem. Phys.*, **100**, 4797 (1994).
73) P. G. Wolynes, *J. Phys. Chem.*, **86**, 5133 (1987).
74) I. Rips, J. Klafter, and J. Jortner, *J. Chem. Phys.*, **86**, 4288 (1988).

75) M. Maroncelli, *J. Mol. Liq.*, **57**, 1 (1993).
76) M. Maroncelli and G. R. Fleming, *J. Chem. Phys.*, **86**, 6221 (1987).
77) M. A. Kahlow, T. J. Kang, and P. F. Barbara, *J. Chem. Phys.*, **88**, 2372 (1988).
78) M. A. Kahlow, W. Jarzeba, T. J. Kang, and P. F. Barbara, *J. Chem. Phys.*, **90**, 151 (1989).
79) K. Tominaga and G. C. Walker, *J. Photochem. Photobiol. A*, in press.
80) H. Pal, Y. Nagasawa, K. Tominaga, and K. Yoshihara, *J. Chem. Phys.*, submitted.
81) E. A. Carter and J. T. Hynes, *J. Chem. Phys.*, **94**, 5961 (1991).
82) T. Fonseca and B. M. Ladanyi, *J. Phys. Chem.*, **95**, 2116 (1991).
83) M. Maroncelli and G. R. Fleming, *J. Chem. Phys.*, **89**, 5044 (1988).
84) R. B. Barnett, U. Landman, and A. Nitzan, *J. Chem. Phys.*, **90**, 4413 (1989).
85) S. J. Rosenthal, X. Xie, M. Du, and G. R. Fleming, *J. Chem. Phys.*, **95**, 4715 (1991).
86) P. F. Barbara, G. C. Walker, and T. P. Smith, *Science*, **256**, 975 (1992).
87) A. M. Kjaer and J. Ulstrup, *J. Am. Chem. Soc.*, **109**, 1934 (1987).
88) F. Markel, N. S. Ferris, I. R. Gould, and A. B. Myers, *J. Am. Chem. Soc.*, **114**, 6208 (1992).
89) T. Tani and S. -I. Kikuchi, *Rept. Inst. Sci. Univ. Tokyo*, **18**, 51 (1968).
90) Z. R. Grabowski, K. Rotkiewicz, A. Siemiarczuk, D. J. Cowly, and W. Baumann, *Nouv. J. Chim.*, **3**, 443 (1979).
91) E. Lippert, W. Rettig, V. Bonacic-Koutecky, F. Heisel, and J. A. Miehe, *Adv. Chem. Phys.*, **68**, 1 (1987).
92) S. Kato and Y. Amatatsu, *J. Chem. Phys.*, **92**, 7241 (1990).
93) R. A. Coveleskie, D. A. Dolson, and C. S. Parmenter, *J. Chem. Phys.*, **72**, 5774 (1980).

Keitaro Yoshihara studied with Profs. H. Akamatu at University of Tokyo and D. R. Kearns at University of California and received Ph. D. from University of Tokyo. In 1965 he joined the research group of Prof. S. Nagakura at University of Tokyo and later at the Institute of Physical and Chemical Research. In 1975 he joined the Institute for Molecular Science at the stage of inauguration as a full professor. In 1988 he was jointly appointed as professor at the Graduate University for Advanced Studies. His research interests include dynamics of electronically and vibrationally excited molecules and primary processes of biologically important molecular systems.

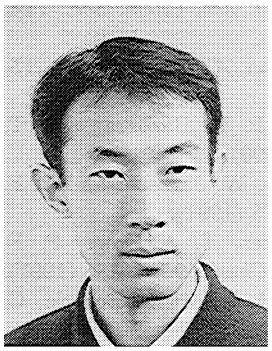

Keisuke Tominaga studied with Prof. Noboru Hirota at KyotoUniversity and received his Ph. D. in 1990. In 1989 he was visiting University of Minnesota to work with Prof. Paul F. Barbara, where he was a postdoctoral fellow from 1990 to 1992. In 1992 he joined the faculty at Institute for Molecular Science. His research interests include chemical reactions and relaxation phenomena in condensed phase.

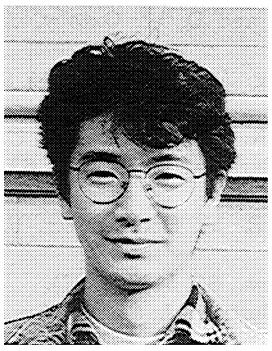

Yutaka Nagasawa received his B. S. in 1989 at Waseda University, where he received his master degree under the supervision of Prof. H. Takahashi in 1991. Then he joined Prof. Keitaro Yoshihara's research group at Institute for Molecular Science, and in 1994 he received his Ph. D. from the Graduate University for Advanced Studies. He is currently working with Prof. Graham R. Fleming at the University of Chicago as a postdoctoral fellow. His research interests include dynamics and structures of electronic and vibrational states.